Mihai D. ROTARU, Jan K. SYKULSKI

School of Electronics and Computer Science, University of Southampton, U.K.

Dual-band electromagnetic band gap structure for noise isolation in mixed signal SiP

Abstract. *A compact dual-band electromagnetic band-gap (EBG) structure is proposed. It is shown through numerical simulation using 3D full wave solver that by adding a slit to the classical mushroom shape an extra resonance is introduced and thus dual-band EBG structures can be built by cascading these new elements. It is also demonstrated that this novel approach can be used to isolate noise in a system such as a dual band transceiver integrated into a mixed signal system in a package. Finally, equivalent circuits have been established to aid the design process.*

Streszczenie. *Przedmiotem pracy jest struktura z przerwą elektromagnetyczną (Electromagnetic Band-gap). Przeprowadzono analizę przy pomocy symulacji falowej 3D dodając dodatkową szczelinę do klasycznego kształtu grzyba i uzyskując dzięki temu dodatkowy rezonans. Pokazano, że nowe rozwiązanie może być używane do izolowania zakłóceń. (**Struktura z przerwą elektromagnetyczną dla izolacji zakłóceń**)*

Keywords: electromagnetic band gap, system in package, electromagnetic noise, noise suppression.
Słowa kluczowe: struktura z przerwą elektromagnetyczną, pakiet, hałas elektromagnetyczny, ograniczenie hałasu.

Introduction

Market demand for wireless systems with more functionality, higher performance, smaller size and lower cost has grown explosively and to meet these expectations the designers have several integration strategies available. In particular, the 'system in package' (SiP) – rather than the 'system on chip' (SoC) – is emerging as a preferred approach as it allows a high degree of flexibility in the package architecture, especially for RF and Mixed-Signal applications. SiP has become the enabling packaging technology platform for wireless communication, which allows the integration of digital ICs, logic ICs and RFICs plus passive components, SAW filters and mechanical parts (Fig. 1). The package is no longer just a connectivity interposer between the IC and the board and has become a system integration vehicle.

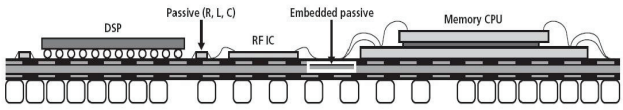

Fig.1. A schematic example of a mixed-signal SiP

In mixed-signal SiP implementations − due to the closely spaced metallic interconnection structures such as traces, vias, pads, leads, partial planes and plane cavities − the coupling of noise generated in the digital side of the system has become a serious signal and power integrity issue. The coupled noise from the fast switching digital devices can affect the phase noise and signal to noise ratio (SNR) of the sensitive RF and communication circuits. One of the major contributors to the high frequency noise is the simultaneous switching noise (SSN) of fast digital circuits such as ASICs and DSPs. There have been various attempts to isolate the SSN coupling between the digital and RF/analog circuits. However, most of the methods offer only a low frequency and narrow band isolation. Over the last few years electromagnetic band gap structures (EBG) have emerged as a complementary solution to isolate the high frequency noise in a wider bandwidth. EBGs are periodic structures that will highly attenuate the electromagnetic waves in certain frequency bands. Several papers have recently discussed the use of high impedance surfaces (HIS), alternate impedance electromagnetic band gaps (AI-EBG) and other EBG structures for suppression of SSN [1, 2]. Different approaches have advantages but also drawbacks; however, those have been discussed elsewhere and are not the subject of this contribution. Recently, a double-staked EBG (DS-EBG) was introduced for low temperature co-fired ceramic (LTCC) multilayer substrates [3]. The purpose of the double staking is to enlarge the bandwidth of the EBG structure without increasing the size of the area occupied by the EBGs. Using this method a 30dB stop-band over X/Ku band range was demonstrated recently [3]. However, the DS-EBG has a disadvantage of an extra layer that has to be integrated during the fabrication process which might be expensive for a low cost system.

In this paper a different approach is proposed. Instead of covering a large bandwidth, the EBG structure is designed to have a dual band such that the two stop-bands can efficiently isolate the frequency bands of interest. This method will keep the effective area occupied by the EBG structure to be the same or slightly smaller than the DS-EBG. Furthermore, the proposed novel dual band structure has features that can easily be changed at the design stage that will allow tuning. By changing different variables of the design without modifying the total area occupied by the structure the designer can tune the frequency bandgap. In [4] a compact SiP X/Ku-band transceiver was designed using the LTCC technology, where the Ku-band transmitter had the centre frequency 14.5GHz and the bandwidth 500MHz, while the X/Ku-band receiver had the centre frequencies 9.25GHz and 14.25GHz, respectively, and a bandwidth of 500MHz. Our suggestion is that a dual stop-band with a bandwidth of at least 500MHz around the 9.25GHz and 14.25GHz, respectively, will be sufficient to efficiently isolate the sensitive RF front ends of the transceiver.

Novel Dual-Band EGB

The proposed structure is based on the classical mushroom shape introduced by Sievenpiper in 1999 [5] with a slight but important modification, namely that a slit has been introduced in the top part of the EBG as shown in Fig. 2. The aim of this study was to design an EBG structure that would work for the same SiP X/Ku-band transceiver as described in [4] but would have only 3 metal layers while occupying similar surface in the SiP transceiver. As shown in [3], the DS-EBG has a much larger band-gap bandwidth than the classical mushroom EBG, mainly because of the staking of two mushroom type EBGs, one from the bottom plane and the other one from the top plane, so that both contribute to the overall band-gap bandwidth. It could be argued that a DS-EBG is effectively a dual-band EBG but

with the property of the two bands being close enough to create a wide continuous band-gap. In this double staking arrangement the area occupied by the structures is not enlarged; however, an extra layer and supplementary vias have to be introduced to achieve the band-gap enhancement effect, thus resulting in a more expensive SiP.

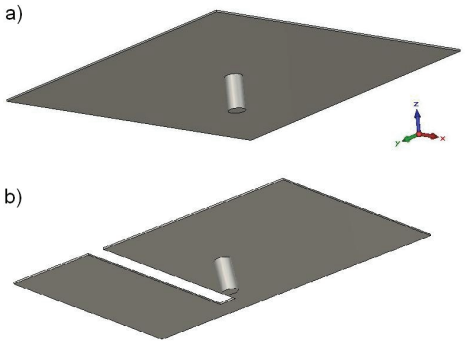

Fig.2 Geometry of the classical (a) and slit-top mushroom (b) EBG elements

Because the EBG unit studied here is a modified version of the classical mushroom EBG unit, it was found useful in the design and associated analysis to use the classical structure as a staring point. To determine and analyse the characteristics of the new EBG structure a simplified test model was built and simulated using CST Microwave Studio [6]. The test structure is based on a microstrip line underneath which the EBG structure is embedded (Fig. 3). Using this methodology allowed better understanding of the behaviour of the EBG and its band-gap characteristics. This approach has another advantage that the model is very simple and thus numerical simulation is fast; once the required design has been found a more complex and time consuming simulation at system level with many coupled EBG structures may be performed. The substrate on which the microstrip line is designed is assumed to be a low loss LTCC substrate with a dielectric constant of 7.4 and thickness t = 0.31 mm. For this configuration a 50 Ω characteristic impedance microstrip line will have the width w = 0.36 mm. The metallisation layer is 10 μm thick and considered lossless for the numerical experiment undertaken here.

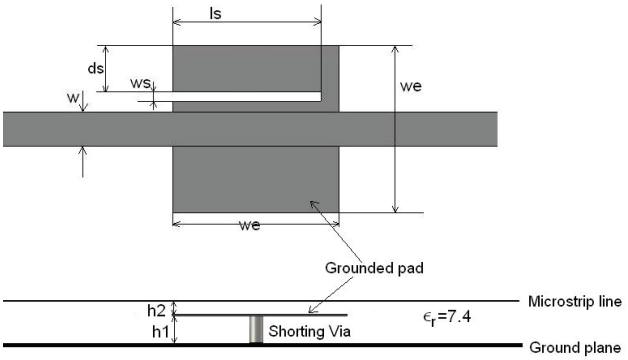

Fig.3 Microstrip line over the slit-EBG structure (top and side views)

The simulation model described above has been built for both the classical and the new 'slit' version of the EBG. For this study the square mushroom top had the width w_e = 1.8 mm, while the distance from the bottom plane was $h1$ = 0.2 mm and the distance from the top plane $h2$ = 0.1 mm. The via diameter was 0.1 mm and was kept constant throughout the study. In this configuration the EBG unit is coupled to the microstrip line and behaves like a notch filter.

In the case of the classical mushroom EBG with the above dimensions and via situated in the centre of the square the simulation has shown a deep notch at 11.33 GHz. This behaviour can be described by an equivalent circuit model formed by a capacitor in series with a parallel combination of a capacitor and inductor (parallel LC tank –fig 4b). The series capacitor describes the electric coupling that exists between the top microstrip layer and the EBG. The LC parallel tank describes the inductance of the via and the electric coupling between the bottom ground plane and the EBG. As shown in Fig. 4a the equivalent circuit description approximates rather well the full wave simulation results in both magnitude and phase. Using this equivalent circuit the equivalent impedance may be calculated as

$$Z = \frac{1-\omega^2 L_{via}\left(C_{top}+C_{bottom}\right)}{j\omega C_{top}\left(1-\omega^2 L_{via}C_{bottom}\right)} \tag{1}$$

It can be deduced from (1) that Z becomes zero when frequency is

$$f = \frac{1}{2\pi\sqrt{L_{via}\left(C_{top}+C_{bottom}\right)}} \tag{2}$$

and thus a short circuit between the microstrip line and the ground has been created. On the other hand Z becomes infinite when frequency

$$f = \frac{1}{2\pi\sqrt{L_{via}C_{bottom}}} \tag{3}$$

These two frequencies (2, 3) correspond to the zero values of |S21| and |S11|, respectively (Fig. 4). It follows from the above analysis that this type of a structure has only one resonant frequency at which Z becomes zero, therefore this type of the EBG can be used successfully to create only one stop-band around this frequency. With these equations one can relate the geometry and the size of the EBG to the resonant frequency. It has to be pointed out here that the extraction of the equivalent circuit parameters values is not a trivial and straight forward task for the mushroom couple to a microstrip case. Because of the field distribution around the mushroom structure a simple static approximation dose not suffice and there are no simple approximations for the capacitance and inductance that work well.

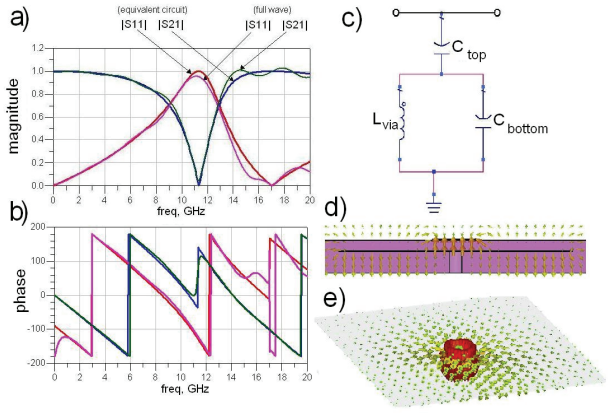

Fig.4 Classical mushroom EBG coupled to a microstrip line. a) Magnitude of scattering parameters (equivalent circuit and full wave), b) Phase of scattering parameters, c) Equivalent circuit model, d) Electric field distribution (full wave solution), e) Current density distribution.

A methodology to extract the values for the equivalent circuit elements has been developed but it will not be presented here as it is not the subject of this work. The interested reader could refer to [7] for more details.

However one of the important results of [7] will be cited here as it shows the nonlinear variation of the L_{via}, C_{bottom}, and C_{top} with size of the mushroom top (Fig. 5). It is interesting to observe that L_{via} has a maximum value but it will drop with further increase in the area of the top of the mushroom, while C_{bottom} and C_{top} will increase but at different rates and eventually C_{bottom} will be bigger than C_{top} (Fig 5).

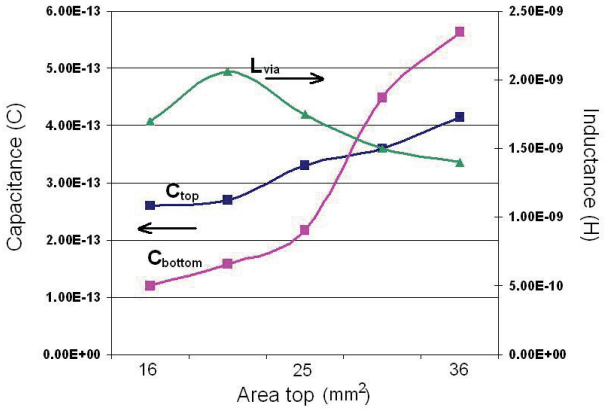

Fig.5. Inductance and capacitance variation with respect to top area for a mushroom EBG coupled to microstrip line

As mentioned in the introduction, for an X/Ku band SiP integrated transceiver that needs noise isolation for its Ku-band transmitter and its X/Ku-band receiver [4] it may be sufficient to provide two stop-bands around the frequencies of interest instead of one very large stop-band. Both the transmitter and receiver need a 500MHz bandwidth around their operating frequencies of 9.25 GHz and 14.25 GHz, respectively. The solution described below could be used not only in the application described in [4] but also in other SiP implementations where the frequencies of interest might be further apart and could not be covered with only one stop-band. As shown before, the classical mushroom EBG is inherently a one stop-band structure and thus to change this feature a slit has been introduced in the top square of the EBG unit as pictured in Fig. 3. The introduction of the slit changes dramatically the current distribution and creates a new dual band response. To understand the behaviour of the new EBG unit, a similar numerical experiment to the one described earlier was undertaken, but now with the slit structure embedded into the microstrip substrate. The simulation results show a much changed behaviour of this structure, namely the presence of two resonant frequencies for which |S21| becomes zero (Fig. 5), one at 9.6 GHz and the second one at 16.15 GHz.

The observed behaviour could also be represented using the equivalent circuit model. However, the new circuit model is not as simple as the one for the classical mushroom EBG. The slit splits the equivalent capacitances C_{bottom} and C_{top} into two components. C_{g1} and C_{g2} are describing now the coupling to the ground plane, while C_{t1} and C_{t2} are used to account for the coupling to the top layer. It is noticeable from Fig. 6 (c and d) that the introduction of the slit changes both the electric field and the current distributions; this phenomenon can be described in equivalent circuit terms as an LC parallel tank formed by L_{slit} and C_{slit}. The L_{via} that describes the via inductance is kept unchanged. Unfortunately, the relationship between the equivalent circuit model components and the resonating frequencies is not as simple as in the previous case. An attempt was made to extract the equivalent impedance of the circuit depicted in Fig. 6b but the resultant formula was found to be far too complex to be of any practical use in design. Therefore, it is recommended for design purposes to employ a numerical full wave solver to extract the characteristics of the slit EBG structure. Notwithstanding, the relationship extracted for the impedance (not quoted here because of its complexity) shows clearly the existence of two resonant frequencies as expected.

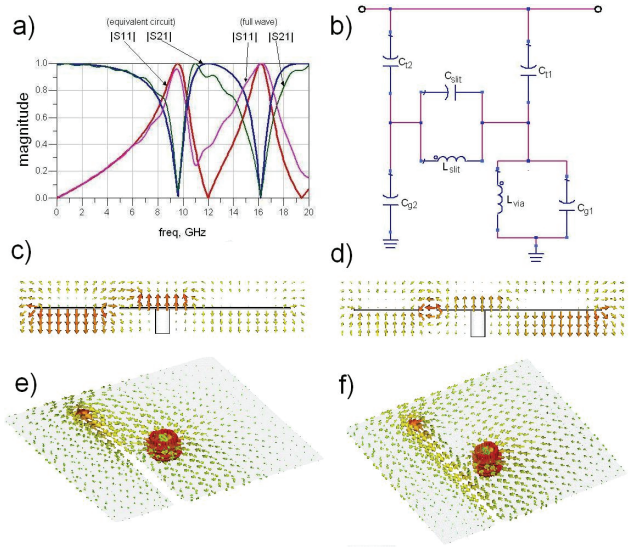

Fig.6. A dual EBG coupled to a microstrip line. a) Magnitude of scattering parameters (equivalent circuit and full wave), b) Equivalent circuit model, c) Electric field distribution at 9.6GHz, d) Electric field distribution at 16.15GHz, e) Current density distribution at 9.6GHz, f) Current density distribution at 16.15GHz

From the equivalent circuit of the slit-EBG unit it can be noticed that, if the ratios C_{g1}/C_{g2} and C_{t1}/C_{t2} are changed, the two resonant frequencies for which |S21| is zero change in a particular manner. If the two ratios are increased, the two resonant frequencies move away from each other – the lower frequency shifts towards lower values whereas the higher frequency increases its value. When the capacitance ratios are decreased, the two resonant frequencies move closer to each other. The change in capacitance ratios can be achieved simply by moving the slit to another position relative to the edge of the top grounded pad (by changing d_s in Fig. 3). This technique can be used to tune the band-gap position; furthermore, by combining EBG units with the slits at different positions the band-gap can be enlarged slightly. Another possibility for tuning the band-gap is to keep its width (w_s) constant and change the length of the slit (l_s) – by doing so the capacitance ratio is varied as well as the values of L_{slit} and C_{slit}. As the length of the slit is reduced the values of L_{slit} and C_{slit} decrease and for a fixed value of w_s there is a minimum l_s for which the slit is efficient. For values below this minimum there is no second resonance and the structure loses its dual band characteristic. If $w_s << l_s$ then the minimum effective $l_s = 0.5 w_e$, where w_e is the width of the top ground pad of the EBG unit. When l_s is varied from its minimum to its maximum value the two resonant frequencies are moved towards lower values; this behaviour can be attributed mainly to the increments in L_{slit} and C_{slit} which result in a drop in the resonant frequencies. The effects of changing l_s and d_s were examined using the full wave simulator and the results in terms of the magnitude of |S21| are presented in Fig. 7 (a and b).

Another interesting feature of this slit-EBG structure can be inferred from Fig. 7 which depicts the variation of magnitude of S21 with frequency. The lower frequency peak is more sensitive to changes in d_s, whereas the higher frequency peak is more sensitive to changes in l_s. In the

example shown in Fig. 7, a 2.5GHz bandwidth for the lower peak was achieved by varying d_s, whereas a 2.4GHz bandwidth for the higher peak was obtained by changing l_s. This property can be exploited in the design of arrays of slit-EBG to enlarge and tune their band-gap response.

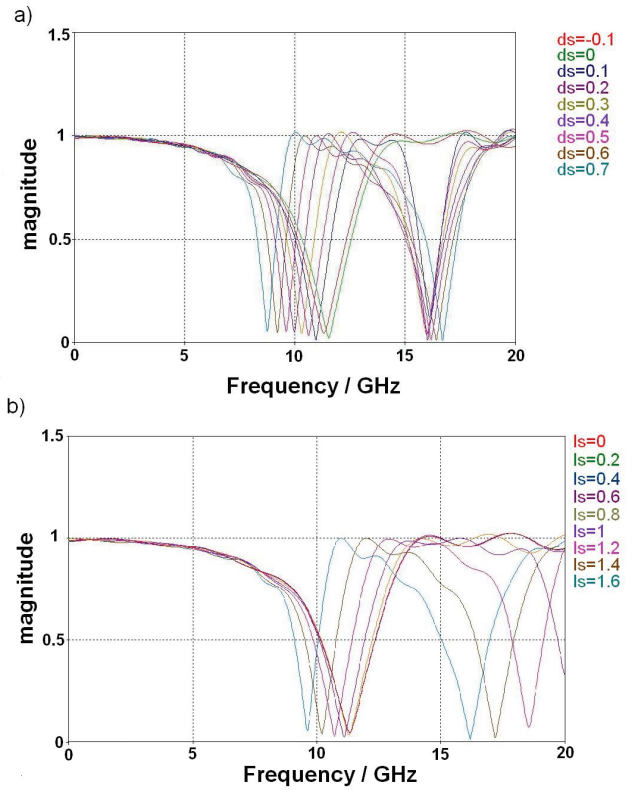

Fig.7. Variation of the magnitude of S21 a) d_s – variable (from 0 to 0.7 mm) (l_s=1.6mm, w_s=0.2mm – fixed) b) l_s – variable (from 0 to 1.6 mm) (d_s=0.5mm, w_s=0.2mm – fixed)

Application of Dual-Band Slit-EBGs in Noise Isolation

In modern electronic systems and products the DC power is distributed throughout the system using parallel plate waveguides (PPW). These metal planes are also used as return paths for the signals. Unfortunately, PPWs allow the TEM modes to propagate, ranging from DC to infinite frequency, as these waveguides do not have an inherent cut-off frequency for the TEM modes. This can be a real problem especially for combined systems where switching a digital DSP can create electromagnetic noise that propagates through PPW as TEM waves and reaches and disturbs the sensitive RF circuitry. Loading the PPWs with EBG structures will create stop bands of frequency throughout which TEM modes are not allowed to propagate, thus creating an excellent way of suppressing high frequency noise.

To demonstrate the efficiency of the proposed new dual band EBG structure, a model with a periodic array of such EBG units between the parallel plate power distribution system of SiP described in [4] has been built and simulated. The transceiver has a 20×20 mm PPW with a 310 μm spacing between the ground and power. The dielectric layer sandwiched between these two metal planes has a dielectric constant of 7.4. The size of the EBG unit is w_e=1.8 mm, with the following slit: l_s=1.6 mm, w_s=0.2 mm and d_s=0.4 mm. The distance between the top metal layer and the top of the EBG unit is 100 μm, while the length of the via is 200 μm and its diameter 100 μm. Three rows of nine EBG units each with a separation of 0.2 mm between neighbouring units were considered. A three-dimensional model of the slit EBG loaded PPW was build and a broad band full wave simulation, from DC to 20 GHz, was performed.

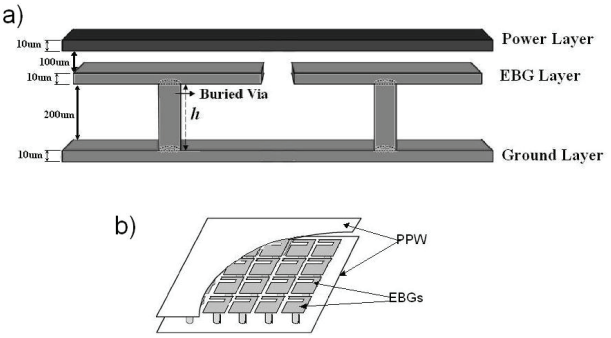

Fig.8. EBG structure within the PPW a) Side view b) 3D View

The results in terms of the magnitude (in dB) of S21 that measures the amount of coupling between Port 1 (position of Ku band transmitter) and Port 2 (position of X/Ku band receiver) are plotted in Fig. 9. The two stop bands are clearly visible and show that any wave propagation will be effectively stopped within the 6.9–9.6 GHz range, as well as within the 13.7–14.9 GHz range. Within these two frequency bands the magnitude of S21 is well below the −30dB 'floor' and therefore the proposed technique can be used effectively to isolate the two sensitive parts of the transceiver SiP described in [4].

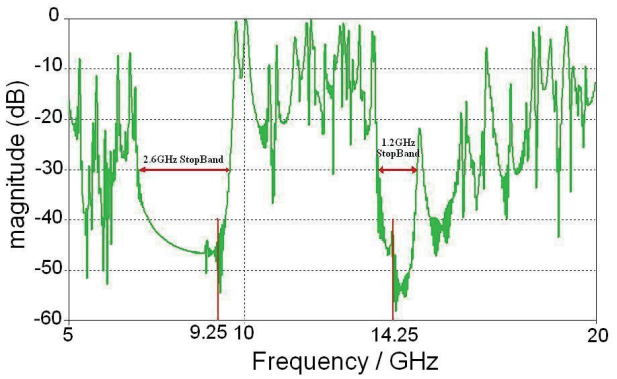

Fig.9. The magnitude of S21 with dual-band EBG structures embedded into the power plane (simulation results)

The effect of combining the slit-EBG structure with controlling position (variable d_s) and length (variable l_s) was also studied at PPW level using the three dimensional full wave model described previously. For the model in which d_s was varied, the width w_s of the slit was kept constant at 0.2 mm, as well its length l_s=1.6 mm. For the three rows of slit EBGs, the following values were selected: d_s = 0.2 mm for the first one, 0.4 mm for the second and 0.6 mm for the third. For this combination it was expected that the lower stop band would be slightly wider than the one for the initially selected value d_s= 0.4 mm for all three rows and that the higher band gap would be largely unaffected. This was confirmed by the numerical model and the new lower effective frequency stop band was now 6.7–9.7 GHz, which 10% wider than the initial frequency band (Fig. 10). The higher frequency band-gap was confirmed not to have changed. For the second analysis of the effects of changing the length l_s, the values kept constant were d_s = 0.4 mm and w_s = 0.2 mm. For this case the lower frequency stop band is slightly wider than for the initial case study; however, the band has been shifted upward and stretches now from 7.2

to 10 GHz. A similar effect has been observed for the upper stop band, its size remaining virtually unchanged but shifted to 14.8 – 16 GHz. It is clear from this numerical exercise that by changing the slot position and size the designer has an effective tool to tune the frequency stop bands to desired positions for a particular design without the need to increase the total area covered by the EBG array.

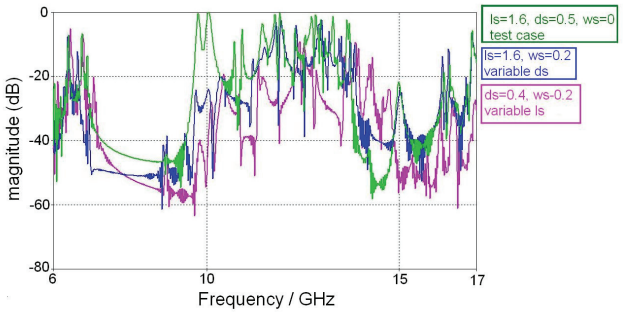

Fig.10. The variation of magnitude of S21 when different design variables of the Dual-Band EBG are modified.

Conclusions

In this work we have investigated, through numerical simulation, the noise isolation capabilities of a novel dual band EBG structure. The proposed slit-top EBG has inherently dual-band behaviour and could therefore be used in systems that need two stop bands. One of the demonstrated features is that the new EBG unit can be tuned by changing the size and position of the slit without modifying the overall size of the cell. This is an important advantage as space is often at a premium in highly integrated electronics systems where this EBG could be applied for noise isolation. The investigation has been conducted mostly using commercial 3D electromagnetic simulation software, however relevant equivalent circuits have been also developed and shown to provide accurate performance predictions, as well as being helpful in aiding understanding of the behaviour of the systems analysed.

REFERENCES

[1] R. Abhari and G.V. Eleftheriades, Mettalo-dielectric electromagnetic bandgap structures for suppression and isolation of the parallel-plate noise in high-speed circuits, *IEEE Trans. Microwave Theory and Techniques*, vol. 51, no. 6, pp 1629-1639, Jun. 2003

[2] Jinwoo Choi, Noise suppression and isolation in mixed-signal systems using alternating impedance electromagnetic bandgap (AI-EBG) structures, *PhD thesis*, 2005

[3] Jongbae Park, Albert C. Lu, Kai M. Chua, Lai L. Wai, Junho Lee and Joungho Kim, Double-Stacked EBG structure for wideband suppression of simultaneous switching noise in LTCC-based SiP applications, *IEEE Microwave and Wireless Components Letters*, Vol . 16, No. 9, pp 481-483, Sept. 2006

[4] Jongbae Park, Junchul Kim, Albert C. Lu, Yujeong Shim and Joungho Kim, Noise isolation in LTCC-based X/Ku-band transceiver SiP using double-stacked electromagnetic bandgap structures, *IEEE International Symposium on Electromagnetic Compatibility*, July 2007

[5] Daniel Frederic Sievenpiper, High-Impedance Electromagnetic Surfaces, *PhD Thesis,* 1999

[6] CST-Microwave Studio – www.cst.com

[7] Rotaru, M. D. and Sykulski, J. K. (2009) Compact Electromagnetic Bandgap Structures for Notch Band in Ultra-Wideband Applications, *17th Conference on the Computation of Electromagnetic Fields COMPUMAG 2009, 22–*26 November, Florianopolis, Brazil. pp. 638-63

Authors: *Dr. Mihai D Rotaru, Prof. Jan K. Sykulski, University of Southampton, School of Electronics and Computer Science, Highfield, Southampton, SO17 1BJ, United Kingdom, E-mail: mr@ecs.soton.ac.uk; jks@soton.ac.uk*